Carleton University
Department of Geography and Environmental Studies

Inuvik Airport Geophysics Investigation: Final Report

Submitted to the
Department of Transportation
Government of the Northwest Territories

Inuvik Airport Geophysics Investigation – Final Report

Report to

Department of Transportation

Government of the Northwest Territories

Attn: Greg Cousineau

Jon Tunnicliffe, Chris Burn,
Carleton University, Ottawa
Department of Geography and Environmental Studies

Alex Becker,
University of California, Berkeley
Earth Sciences Division, Geophysics Department

Patrick Finlay,
EBA Engineering, Ottawa

Koichi Hayashi,
OYO Corporation / Geometrics, San Jose

and Lothar Schrott
Geomorphology and Environmental Systems Research Group, Salzburg
University of Salzburg

September, 2011

Executive Summary

From June 6 to June 13th, an international group of geophysics and permafrost specialists met to carry out fieldwork and evaluate the use of geophysical techniques on airport runways built on permafrost. This was a pilot exercise to support and develop later-stage survey work for the assessment of runway issues related to terrain stability (notably subsidence) and surface hydrology. The site of investigation was Inuvik's Mike Zubko airport (CYEV).

The Inuvik airport makes an excellent test case because there is a good database for the site of ground temperatures, construction details, and geotechnical drilling logs. This enables us to develop an integrated picture of subsurface conditions.

Three geophysical survey techniques were used in the investigation: capacitively-coupled and conventional resistivity (Ohm-Mapper and MiniRes), ground penetrating radar (GPR), and multi-channel analysis of surface waves (MASW). Records from the longitudinal runway profiles show relatively uniform stratigraphy. Results are consistent with drilling logs. Within the data set it is possible to discern a basal till layer overlying bedrock, overlain by peat of variable thickness and a thick (4 m) embankment made of compacted crushed rock. The longitudinal runway surveys reveal fairly uniform conditions. Lateral transects at taxiway Alpha and the Forward Operating Location (FOL) taxiway show more variation: there is evidence of older drainage pathways, resulting in more heterogeneous resistivities, and evidence of deep ground ice.

By overlying data from multiple survey transects, it is possible to extract more information than is possible using a single system. A set of readings from one system that might otherwise be inconclusive can be checked against the corresponding survey results from another. A method of categorization is proposed, based on an integrated analysis of the data collected. Using information from both MASW and resistivity surveys, it is possible to set criteria in order to flag areas of potential concern along the runway transects.

Contents

Introduction

From June 6 to June 13th, an international group of geophysics and permafrost specialists met to carry out fieldwork and evaluate the use of geophysical techniques on airport runways built on permafrost. The site of investigation was Inuvik's Mike Zubko airport (CYEV). The fieldwork was a pilot exercise to support and develop later-stage survey work for the assessment of runway susceptibility to permafrost- and drainage-related issues.

The work provided the opportunity for an evaluation of a suite of geophysical techniques and instruments for finding and monitoring problem areas beneath runways in permafrost zones. It also provided some validation of remote-sensing assessment work that has been carried out on the Inuvik runway. The intention of the work is to develop and enhance the linkages inferred between large-scale terrain classification and finer-scale problems found on runways and associated infrastructure. Through such work we may enhance our capacity for remote evaluation of runway sensitivity to permafrost and surface hydrology issues, thus making it easier to assess a large number of such installations. The Inuvik airport makes an excellent test case, because there is a good database available for the site, such as ground temperature, construction details, geotechnical drilling logs, and some GPR sections from earlier surveys. This enables us to develop an integrated picture of subsurface conditions.

The geophysical techniques deployed were:

- Ground penetrating rader (GPR);
- Capacitatively-coupled resistivity (Ohm-Mapper);
- Galvanic resistivity (Mini-Res).
- Multi-channel analysis of surface waves (MASW);

The fieldwork was conducted between 2000 and 0400 each night at Inuvik Airport when the runway was closed to normal operations. The runway was closed for the duration of the testing. We are grateful to Karen King, Inuvik Airport Manager, for providing safe working conditions and arranging use of a hangar as a logistical base. EBA Engineering provided personnel, GPR and a geophone landstreamer

for the project. Geometrics, Inc of San Jose, CA provided personnel, a GEODE seismograph and the Ohm-Mapper system for the survey work. The Mini-Res system was furnished by L & N Instruments of Lake Tahoe, NV.

The aims were to:

i) develop a detailed subsurface model of Inuvik Airport runway and taxiways. Ice and groundwater flow pathways were to be systematically mapped;
ii) cross-calibrate multiple geophysical survey techniques;
iii) exchange information and experience in emerging technologies, data processing techniques, and linkage of ground conditions to geophysical readings;
iv) move beyond conventional survey techniques. In particular, examine the possibility of 3-D resistivity surveys and the applicability of induced-polarization techniques in frozen ground;
v) lay the groundwork for protocol development for systematic geophysical surveys of multiple airstrips, following airphoto and satellite terrain analysis;

The modified Ohm-Mapper interface required for the full 3-D resistivity surveys (point *iv*) proved problematic to implement. As an alternative, multichannel analysis of surface waves was investigated (MASW; Park *et al*., 1999; Hayashi and Suzuki, 2004; Park and Miller, 2004). The results provided key parameters for evaluating the stiffness of near-surface strata, and a good picture of shallow (2-10 m) surface stratigraphy at Inuvik Airport.

Geotechnical Setting

The Airport site is underlain by permafrost and ice-rich frozen soils. The thickness of permafrost in the Inuvik region is 90 m (Burn *et al*. 2009). In the 1960s, mean annual ground temperatures were estimated to be approximately -3°C, but more recently higher temperatures have been measured in undisturbed ground (-1.6°C). The proximity of permafrost to thawing temperatures is remarkable this far north of the southern limit of permafrost.

The active layer above the permafrost at the Inuvik townsite varies in thickness from 0.5 to 2.5 m. At the airport, the thickness varies somewhat less, from about 45 to 120 cm (EBA, 2002). The site remains relatively cold during winter because the runway is cleared of snow. Following runway construction the ground beneath the embankment remained frozen throughout the year. At present, there is no data from the airport site available to establish whether this equilibrium has remained intact.

The runway is 1830 m long and 46 m wide, with 23 m shoulders. Taxiways is 23 m wide with 15 m shoulders. The runway has a pavement loading rating of 11 (out of 12), meaning it can accommodate relatively large, heavy aircraft. The airfield was designed to prevent or minimize thawing of the underlying frozen ground, and consists of a thick embankment of rock fill (average 3 m thickness, up to 4.2 m) placed on the undisturbed ground surface. Insulation was not used in the construction of the runway and taxiways, although some has been installed in places, such as the taxiway for the Forward Operating Location (FOL) base. The upper 23 cm of the fill is a crushed gravel base, which is capped in turn by asphalt-concrete, approximately 9 cm thick (Figure 1).

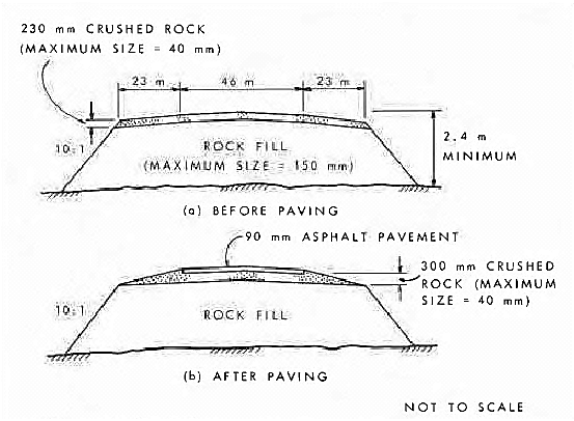

Figure 1- Typical cross sections, Inuvik Runway. From Johnston (1982).

Depths to bedrock at the Airport site are variable. Reported depths range from 1.6 to 3.1 m (EBA, 2002) to over 10 m (AMEC, 2010). One borehole, sited 400 m beyond the eastern end of the runway (site 6: AMEC BH-02) reached bedrock at 10 m, while others finished at similar depths without encountering bedrock. At the western end of the runway, bedrock was intercepted at 3.1 and 2.9 m, 400 and 700 m beyond the paved runway, respectively.

A gray silty gravel of unknown thickness underlies most of the study area and is interpreted as a basal till. A brown silt (1.5 to 3.3 m thick) with varying amounts of sand, clay and stones sits upon this till. The silt layer contains ice up to 60 cm thick near the top of the unit. Horizontal ice lenses, up to 2.4 cm thick have been found throughout the unit. The uppermost layer consists of organic material varying in thickness from 0.1 to 2.4 m (Johnston, 1982).

A terrain map based on historical imagery of the study site (see Tunnicliffe and Burn, 2011) is shown in Figure 2. **Former alluvial drainage channels (F)** in the study area appear as low-lying troughs filled with fine-grained alluvium and organics. These can be distinguished in airphotos by their contrasting vegetation. They were most likely formed in postglacial times and, prior to airport construction, acted as preferential flowpaths, conveying surface runoff. These features link together the smaller lakes and active drainage channels that lead to Limestone (Airport) Lake.

The study area has numerous small lakes: two were infilled in the course of runway construction, one at the east end and one at the west end of the runway. Evidence of older **lacustrine (L) deposits** can be seen in historical airphoto imagery. Most of the remaining terrain is classified as **moraine (M)** of either shallow (**v**) or intermediate (**p**,**k**) depth.

Methods

The investigation used four different instrument setups on 12 profile segments across the study site, namely:

- three long runway profiles;
- five transverse sections;
- two taxiways;
- two of the proposed extension centerlines.

Notes were made of drainage conditions and any sites that were subject to cracks, undulation, subsidence or other deformation. Profile lines that had been surveyed by Judge *et al*. (1991) in their GPR study of the Inuvik runway were re-surveyed, and results compared. Roughly 50 km of lines were covered in multiple surveys over the course of the eight nights.

Two sites of major subsidence, well-known to those who work on the runway, were noted during the survey: (1) a major dip near the intersection of the Forward Operating Location (FOL) taxiway and the east end of the runway, and (2) on the north side of the runway, 300 m from the east end of the runway (Figure 2). Detailed transects of these sites were carried out in order to assess the geophysical contrast between ground that is undergoing subsidence (Figure 3) and the surrounding terrain.

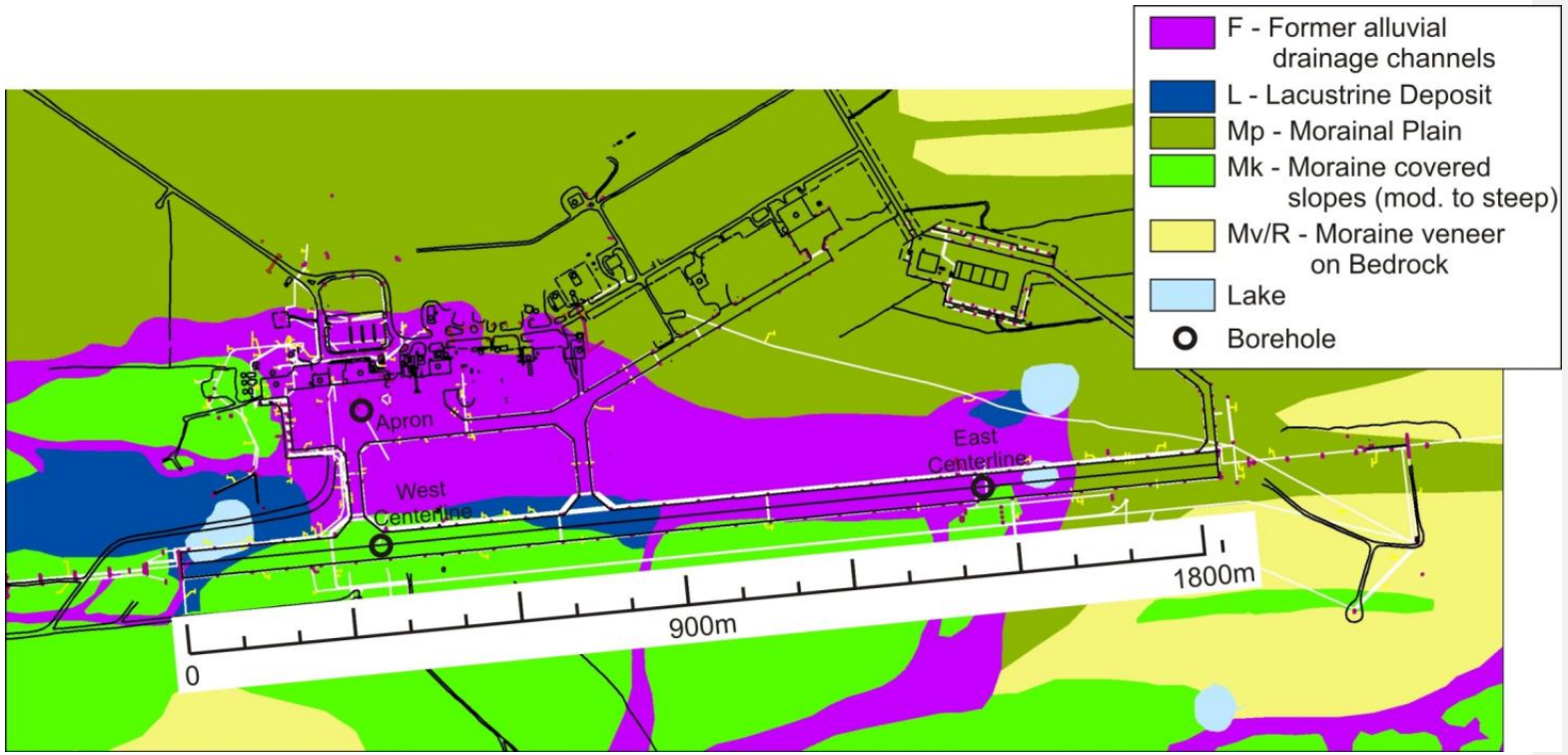

Figure 2 - Long profile map, showing terrain units inferred from historical airphotos. Buried cabling and conduits are shown in white. Boreholes are indicated as black circles. The runway is 1828 m (6000') in length.

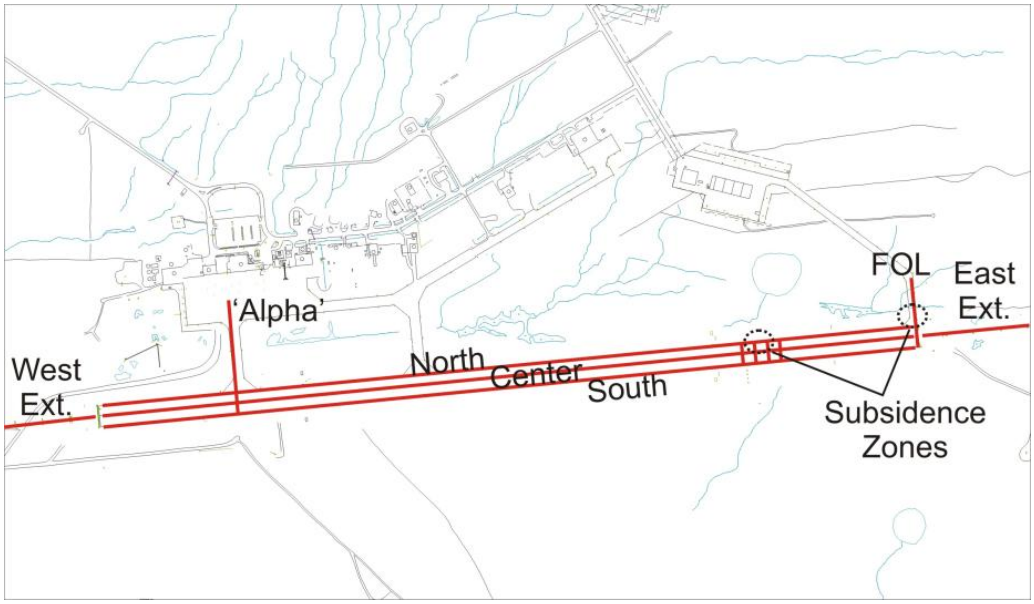

Figure 3- Schematic of the Inuvik Airport survey layout. Red lines indicate survey profiles carried out using GPR, Ohm-Mapper and MASW. Dashed circles indicate subsidence zones.

Resistivity Surveys

Resistivity measurements from the Geometrics OhmMapper TR-5 were used to assess the physical parameters of the subsurface materials – resistivity is a function of water saturation or ice content, dissolved minerals in interstitial water, porosity, grain size and temperature (refs). Resistivity techniques work well in permafrost regions because of the marked increase in electrical resistivity of water that occurs as it reaches the freezing point. Resistivity will vary directly as a function of the ice content and type; for example, sediments with low ice contents are generally conductive and typically have low resistivities. Sediments with high ice contents will generally have resistivities higher than sediments without ground ice but lower than sediments containing massive ice.

Geometrics' OhmMapper has a simple coaxial-cable array with transmitter and five receiver sections that are pulled, in this case by a vehicle, along each runway transect. The system is unique in that it does not require direct coupling with the ground; in a capacitively-coupled resistivity meter the

transmitter uses the capacitance of an antenna to couple an AC signal into the ground. Data collection is many times faster than systems using conventional DC resistivity. A series of measurements are made along a profile by towing the array with a constant transmitter-receiver separation.

Each runway or taxiway transect was covered three or four times with successively longer dipole lengths and transmitter spacing, permitting increasingly deeper subsurface penetration. The capacitance of the cable is determined primarily by the length of the cable, where a longer cable has a greater capacitance, and thus the capability to couple more current into the ground. The longest array (20-60-20, Table 1) extended 228 m, and proved impractical for shorter sections. Multiple survey lines with different geometry setups were integrated to provide a single detailed profile of resistivity to a depth of up to 25 m.

Table 1 - Geometry of OhmMapper survey lines. Geometry is shown as x-x-x, where the first and last numbers represents the length of the receiver and transmitter dipoles, respectively; the middle number represents the spacing between the transmitter and the first receiver dipole as well as the spacing between it and the subsequent receiver dipoles.

Received Geometry	Approx Depth (m)	Long runway	Taxiway Alpha	FOL Taxiway	Proposed Extensions
5-5-5	1.4 - 4.2	x	x	x	x
10-5-10	2.6 - 5.3	x	x	x	x
20-10-20	5.2 - 10.5	x	x	x	
20-60-20	15 - 25	x			

Data processing involves application of an appropriate inversion algorithm using the set of resistivity measurements to determine the most probable 2D (distance and depth) resistivity structure of the ground along the survey line. Resistivity inversion is an iterative process that attempts to reduce the difference between the calculated and measured apparent resistivity values by adjusting the resistivity of each block in a model grid (Loke *et al*., 2003). Different models may arise from the same set of measurements, depending on the inversion algorithm and relevant parameters, such as the initial earth model, grid resolution or the least-squares criterion employed. Because of this indeterminact, the data processing used here is really a transformation. Qualitative interpretation of the record involves comparison of the results with published values (c.f. Figure 4) or, optimally, with drilling records from the study site.

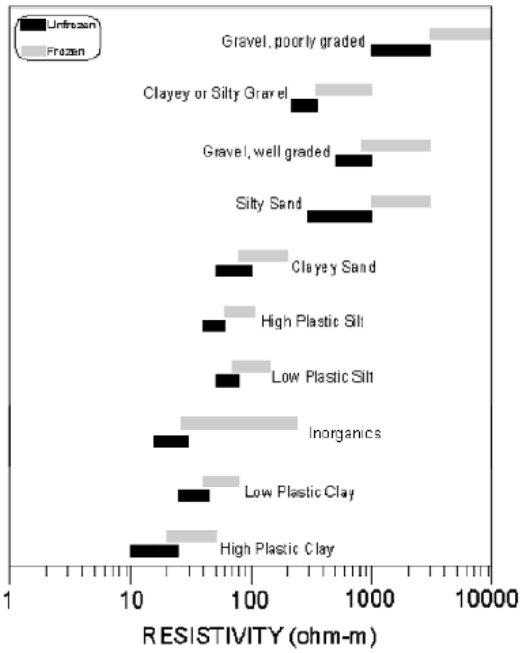

Figure 4 - Typical resistivity values for a variety of earth materials; when the ground temperature is below 0°C, higher resistivity results. Henderson, n.d..

MiniRes Measurements

Galvanic measurements are a more traditional method of measuring the resistance of earth materials (Telford, 1990; Reynolds, 2006). In galvanic surveys, an array of metal spikes are driven into the ground, and the electrical potential amongst the electrodes is measured. For this survey, an L&R Instruments MiniRes was used to conduct a Wenner array-type survey at five different sites in order to calibrate the resistivity readings from the OhmMapper. The process of data inversion is identical to the OhmMapper, though the measurements were taken only at a single site, rather than a long transect. The results are thus 1-D (depth) rather than 2-D (depth and distance along the profile).

Ground penetrating radar (GPR)

GPR is used to assess stratigraphic boundaries and structures in the subsurface. It uses the transmission and reflection of high frequency (1 MHz to 1 GHz) electromagnetic waves, typically polarized, within the earth. Each measurement involves a short pulse or "wavelet" of EM energy transmitted to the ground. The transmitting antenna acts as a band-pass filter, emitting sine waves with a center frequency determined by the antenna. The reflected energy is returned to the surface and recorded at the receiver antenna (Knight, 2001).

Penetration depth of a GPR signal depends on the antenna frequency in combination with the dielectric constant (ε) and the electrical conductivity (σ) of the subsurface materials. Conductive materials are generally opaque to EM waves. High water and/or clay contents (high ε, high σ) leads to a stronger attenuation and, therefore, a markedly reduced penetration depth (e.g., <5 m). In drier and more electrically resistive materials, penetration depths of between 30 and 60 m can be achieved.

EBA Engineering provided their Mala Ramac GPR unit with 50, 100 and 500 MHz rough terrain antennas for the survey work. The antennas were towed by a vehicle along the runway and taxiway transects.

GPR data were processed using the signal processing suite within Octave, an open-source MATLAB-type numerical processing software. Filtering, gain and topographic correction were applied to the GPR traces. In the subsurface, the pulse travels at a velocity that depends on the electrical properties of the subsurface material. This velocity will be some appreciable fraction of the speed of light, typically varying from 0.05 to 0.16 m ns-1, higher in frozen or dry soils and lower in wet materials. The velocity of the wave is represented thus:

$$v = {c_0}/{\sqrt{\varepsilon_t}}$$

where v is the electromagnetic wave velocity, c_0 is the speed of light in free space, and ε_t is the relative dielectric permittivity constant.

Table 2- Typical values for the dielectric constant and velocity for common geological materials at 100 MHz (DePascale et al. 2008)

Material	Dielectric Constant	Velocity (m/ns)
Dry sand	3–5	0.15
Ice	3–4	0.16
Frozen sediment	6	0.12
Saturated sand	20–30	0.06
Fresh water	80	0.033
Seawater	80	0.01

Common mid-point (CMP) surveys carried out by Judge *et al*. (1991) suggest that the subsurface wave velocity at Inuvik is 0.08 $m \cdot ns^{-1}$, which we have adopted for our calculations of GPR penetration depth. There is likely to be variation in this parameter, both vertically and laterally, but the associated uncertainty in interpreted depth is likely to be less than 15%.

The radargrams from the 50 MHz and 100 MHz antennas were generally of poor quality, with little resolved detail. The best imagery was obtained using the 500 MHz antenna. Antenna choice presents a tradeoff between depth of penetration and the resultant resolution: the 500 MHz antenna typically has lower penetration, but much higher resolution.

Interpretation of the GPR record involves both qualitative and quantitative interpretation of the recorded information. Optimum imaging is achieved when there are at least a few sharp stratigraphic boundaries and good contrast amongst the geotechnical properties of ground materials. The reflectivity at a layer boundary is determined by the contrast in the dielectric properties of the subsurface units. The higher the difference between the refraction indices of the two media, the greater the reflected energy. Smaller-scale differences in water content and/or grain-size composition can potentially yield stronger reflections than larger-scale stratigraphic contacts. The processed radar data can thus be used in a qualitative way to obtain information about the structure and stratigraphy of the subsurface and to locate regions of anomalous EM properties.

Multichannel analysis of surface waves (MASW)

MASW is used to assess the seismic velocity of shear waves within the surface strata of the investigation site (Park *et al*., 1999; Hayashi and Suzuki, 2004; Park and Miller, 2004, 2007). Measurements of shear wave velocity (v_s) provide key parameters for evaluating the stiffness and competence of the subsurface medium, and a good picture of shallow (2-10 m) surface stratigraphy. The 'active' MASW technique employed at Inuvik involves using a sledge hammer source and an array of 4.5 Hz vertical geophones with base plates, spaced at 1 m intervals (Figure 5,6). Surface wave data was collected in a 'roll-along' acquisition fashion, moving the array 10 m between shot setups (5 m on some of the shorter taxiway and runway cross section surveys). 'Passive' mode MASW involves leaving the geophone array on the ground for an interval of 20-30 minutes to record background vibrations from the local environment – this method was attempted at the runway, but did not yield satisfactory results.

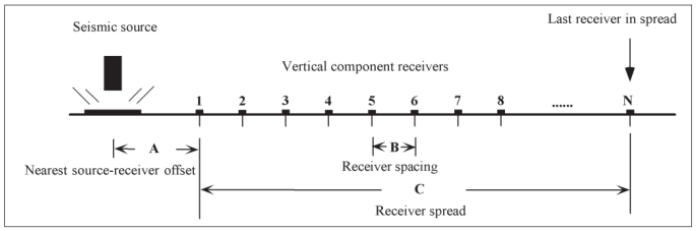

Figure 5 - MASW survey layout. From Xia et al., 2002. The Inuvik survey used a 24 channel land streamer with 1 m spacing between electrodes.

Rayleigh waves are surface waves that travel along a free surface, such as the earth-air interfrace. They are the result of interfering P- and S-waves, and have traditionally been viewed as noise (Miller *et al*. 2004). Recent advances in processing surface wave data has resulted in the development of a promising technique for engineering studies. Longer wavelengths penetrate deeper than shorter wavelengths for a given mode, generally exhibit greater phase velocities, and are more sensitive to the elastic properties of the deeper layers. Shorter wavelengths are sensitive to the physical properties of surficial layers. For this reason, a particular mode of surface wave will possess a unique phase velocity for each unique wavelength, lending to the dispersion in the seismic signal. Figure 7 shows an example of 'picking' the dominant velocity at each frequency to construct the dispersion curve.

Figure 6- Deployment of the geophone land streamer at the east end of the runway centerline.

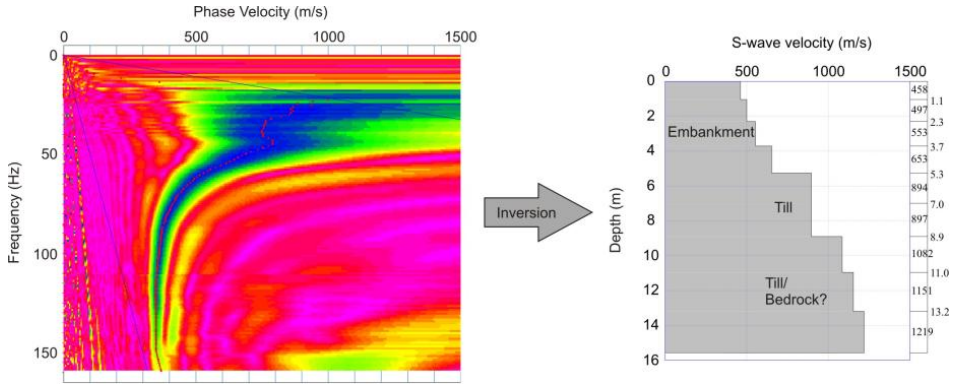

Figure 7- An example of MASW processing. The phase velocity-frequency plot shows the trend of dominant phase velocities for each frequency. The peak values (curved, dark blue band) are selected to outline the 'dispersion curve' for each array setup (Geometrics,2009).

Results from dispersion curve development are then used for inversion of the ground model, producing an estimate of the subsurface stratigraphy. 2-D S-wave velocity sections are generated with gridding software by placing each S-wave profile (*V*s versus depth) in the middle of the geophone spread with which it was calculated.

As with the interpretation of resistivity data, results from the inversion model are compared with published values or with calibrated data from boreholes in the study area. The largest compilation of seismic velocity readings in formerly glaciated settings comes from Hunter (2007): trends highlighted in Figure 8 show that seismic velocity generally increases with depth, due to compaction and decreasing porosity, and accompanying increase in bulk moduli and shear moduli. The database includes both Holocene and Pleistocene age sediments - in general, Pleistocene materials exhibit overall lower porosity that Holocene materials at a given depth due to consolidation.

There is little reference in the literature to MASW usage in ice-rich terrain, and thus the shear wave velocities in permafrost are not well characterized. It is anticipated, however, that zones with significant ground ice content will show higher velocities and good contrast with the surrounding terrain.

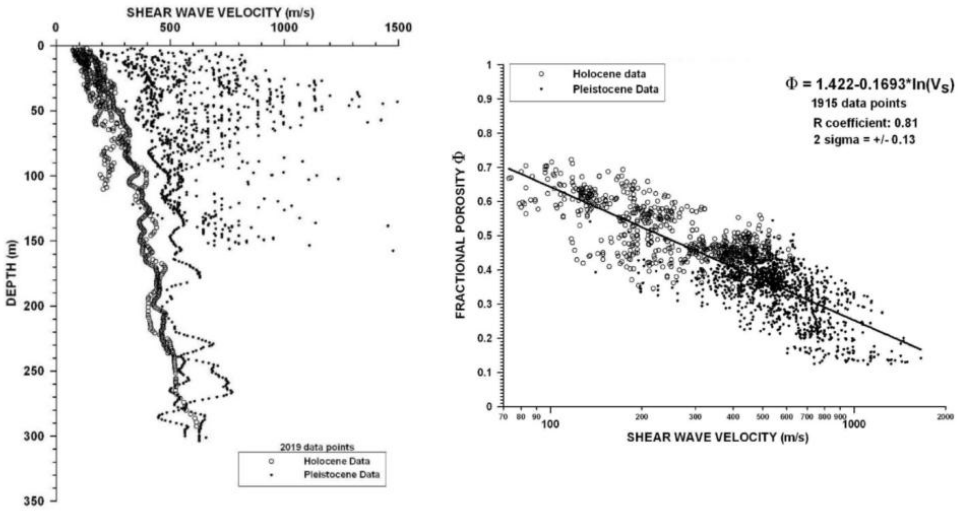

Figure 8- from Hunter (2007). A compilation of seismic velocity (Vs) readings, comparing Vs with (a) stratigraphic depth and (b) fractional porosity.

Results

Review of the geophysical logs reveals that most of the study area has a relatively uniform subsurface composition. The runway embankment, up to 4 m thick, overlies a peat layer of variable thickness and ice content. Drilling logs from Johnston (1982) reveal some sandy layers and a stony clay silt till at depth (see Geotechnical Setting, above).

Results can be best interpreted by comparing geophysical results to the drilling logs: three borehole logs are presented in Figure 9 with accompanying survey data from the corresponding borehole sites. Galvanic resistivity readings were taken on the north shoulder near the centerline east borehole (Figure 9) to confirm the trend in resistivity values with depth. The embankment layer shows high resistivity (>1000 Ω-m), and consistently layered, large amplitude waves in the GPR trace. The MASW data shows a readily discernible contrast between shear wave velocity (*V*s) in the embankment material and layers below.

The peat layer beneath the embankment typically stands out as a wavy, disordered GPR signal of varying thickness and lower resistivity than the overlying crushed rock material. GPR reflectors are weaker or interrupted in places where the presence of ground ice imparts a different dielectric character to the substrate. This is especially evident in the apron subsurface (Figure 9c) – see the description of Taxiway Alpha, below. Where the peat layer is thin and compacted, it does not present sufficient contrast to be resolved by the GPR and the MASW surveys.

The underlying till layers can sometimes, but not always, be distinguished from the overlying peat by higher resistivity values (200-1000 Ω-m) depending, most likely, on ice content. The till does not show significant seismic layering in the GPR record, and presents little contrast in the MASW record. The peat and till package ranges between roughly 6 and 15 m in total thickness. The till-bedrock interface is probably within range of the surveys, but there is rarely a strong enough contrast shown in any of the geophysical records to state definitively where the boundary lies throughout the study area.

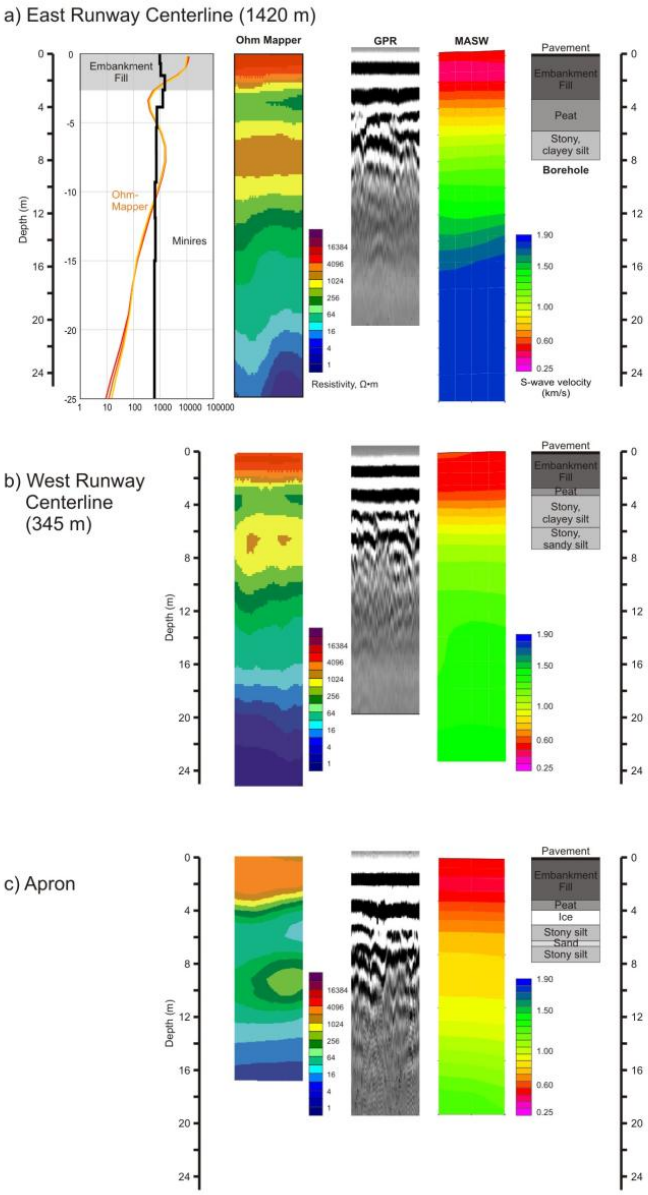

Figure 9- Three borehole logs (Johnston, 1982) are compared with geophysical soundings at each site: results from OhmMapper, GPR and MASW are compared.(a) Runway Centreline East, located at 1425 m along the runway centerline, (b) Runway Centreline West, located at 325 m along the runway centreline and (c) Apron site. At the latter site, the borehole is approximately 25 m from the end of the geophysical transect, so it should be considered a generalized comparison.

Interpretation: Overlaying Geophysical Datasets

By overlying data from multiple survey transects, it is possible to extract more information than is possible using a single system (*e.g.* DePascale *et al*., 2008). It is important to develop a systematic understanding of the multiple seismic and resistivity indicators in order to most effectively interpret the structure of the subsurface. An example is shown below (Figure 10, see also Figure 12), focusing on the easternmost 400 m along the northern runway edge, before the FOL taxiway.

For the present purposes, the most important aim is to identify likely concentrations of ice or ice-rich sediment within the subsurface, as well as other information on sites of past or potential subsidence. Combining the OhmMapper and GPR results (Figure 10a) helps us to distinguish, to some extent, what is massive ice and what may be considered more dispersed concentrations of segregated ice or ice lenses within the sedimentary layers. GPR traces within clear massive ice tend to have a sharp upper boundary and a clear, reflection-free signal (e.g. Moorman *et al*., 2003) while diffraction of the GPR signal in segregated ice and ice lenses leads to much noisier returns. Most of what we see in the Inuvik runway record is labeled as ice-rich sediment; there are few anomalies that have sufficiently high resistivity to be considered massive ground ice. GPR also provides some indication of collapse structures, folds and faulting within the sedimentary layers. Many such features are related to adjacent to ice-rich bodies.

The addition of MASW information helps to distinguish between competent frozen ice mass and more dispersed ice content, though at a lower resolution. There is a consistent pattern of low-to-high S_v with increasing profile depth, due to compaction. Distortions of this gradient are typically due to the presence of ice (high S_v) or to more loosely consolidated substrate such as organics (low S_v). Figure 10b shows the MASW contours overlying the resistivity data. The high-resistivity anomaly on the right (roughly 1740 m) is associated with a low-velocity zone within the peat strata. Presumably, this area of ice-rich organics is not as compacted as the adjacent materials.

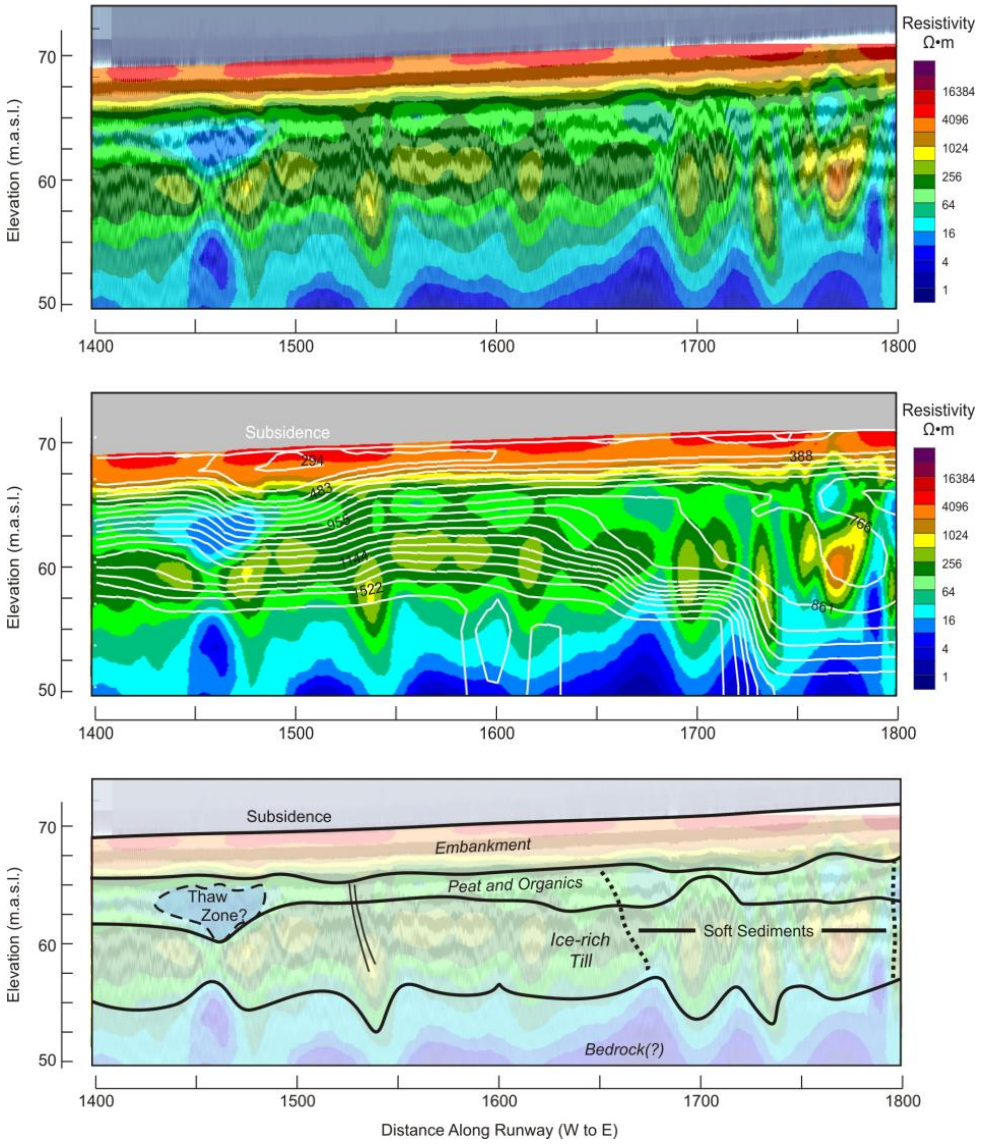

Figure 10 - (a) Resistivity and GPR overlay, (b) Resistivity with MASW shear velocity contours, and (c) interpretation of overlaid datasets. The top stratum is the runway embankment, overlying peat and organics with till below.

Figure 10c shows the final interpretation of the combined geophysical data. Zones of high resistivity and strong GPR layering are assumed to be ice-rich till. A low-resistivity anomaly at roughly 1440 m is interpreted to be an area of possible thaw. This may be associated with the subsidence a short distance to the east. The subsidence zone at surface appears only in the MASW data. A zone of less consolidated sediments is indicated on the left, based on the MASW data. It is worth emphasizing again that this integrated diagnostic picture would not be possible without the benefit of multiple data sources.

Runway – Long Profile

The longitudinal OhmMapper records (Figure 11) show a consistent embankment fill thickness, and a more variable peat/till thickness along the length of the runway. The North and South profiles show greater affinity with each other than with the centerline: this may reflect either (1) enhanced freezing conditions at the centreline, or (2) some geophysical edge effects resulting from off-line influences such as high embankment shoulders. The receivers were not shielded, so there may be some influence from the exposed sideslopes and also from lighting fixtures and cabling along the runway shoulder.

There is a deeper zone of highly resistive, likely frozen, materials between 1200 m and 1500 m along the profile, which generally coincides with the alluvial 'flow channel' terrain unit, indicated in Figure 2. Drill logs from this portion of the runway indicate significantly thicker accumulations of peat (>2 m) than at the west end of the runway (<1 m, Figure 9). Proximity to terrain units with shallow 'veneer' attributes to the east suggests a gradual shallowing of bedrock depths in that direction.

Cabling, ducts and culverts are likely to show a strong resistivity response, though this signal may be masked somewhat in the highly resistive embankment. Circles with a cross in Figure 11 indicate the locations of known wiring and drainage conduits, based on 'as-built' diagrams of the airport. It is possible that more recent fixtures have been installed. Other major resistive anomalies likely represent ice bodies within the substrate.

At the eastern end of the runway (north transect, Figure 12), the three different survey techniques highlight some interesting characteristics of the subsurface. The 500 MHz GPR record shows relatively uniform bedding along the runway, except for a few isolated anomalies that generally align with anomalies within the resistivity and/or MASW profiles.

A deep zone of low-velocity material is evident at the eastern end, under the runway threshold. This corresponds with a zone of relatively high resistivity in the OhmMapper record, and some indications of ice within the GPR record. This zone has proven problematic for the FOL taxiway (see below), having caused significant subsidence at the intersection of the taxiway and the northern edge of the runway.

Further to the west, there is a deep (~12 m) anomaly visible within the MASW record, also clearly visible in the radargram. The origin of this feature is unknown, but probably related to ground ice conditions. There is no evidence of any distortion of the embankment or runway surface.

During the survey, there was a distinct subsidence patch noted near the 1000 ft. marker (survey chainage 1525 m) on the north edge of the runway. Of the three survey methods employed, MASW provides the best characterization of this `soft spot'. The anomaly is close to the surface, mainly within the embankment material; it does not stand out in the OhmMapper record, and there is only some slight distortion on its eastern edge evident within the GPR record. Figure 13 (top) shows the results from several MASW cross sections, used to map out the extent of the soft spot. The surficial extent of the subsidence (deformation and cracking) was estimated to be 25 m long and 10 m wide at the time of the survey (Figure 13, bottom); the results show the disturbance extending at least 50 m along the runway and perhaps 30 m toward the centerline of the runway.

Figure 11- (next page) Ohm mapper surveys running from West to East. The eastern half of the runway shows a large-scale high-resistivity zone. Spikes of high resistivity values may be buried pipes, cabling from light installations along the runway. Records from the deepest soundings tended to be noisier, leading to some anomalous values at depths below 8-10 m.

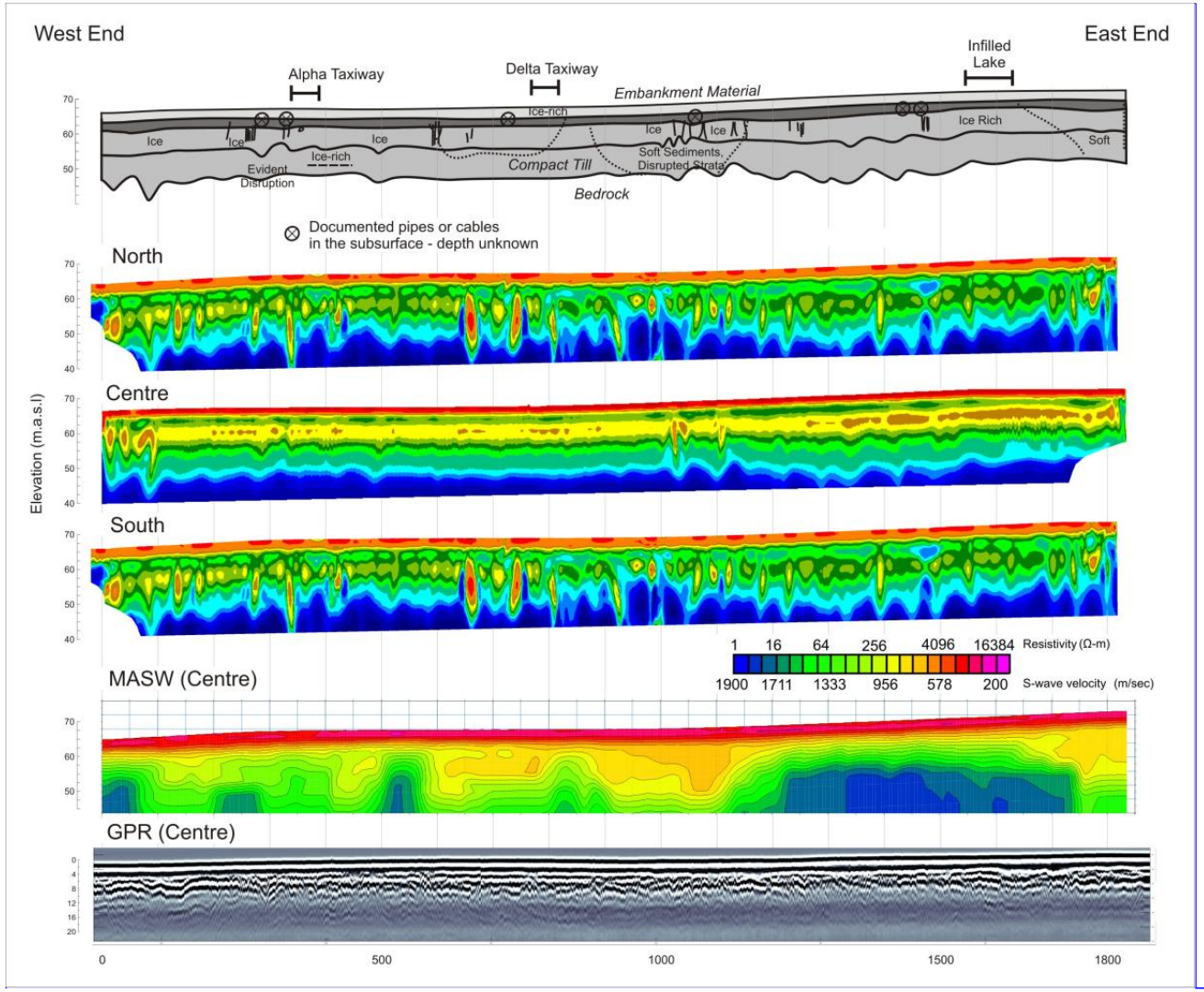

Comment [JFT1]: Note the South transect is just a repeat of the North transect (they are similar). New processing is being done for the South transect.

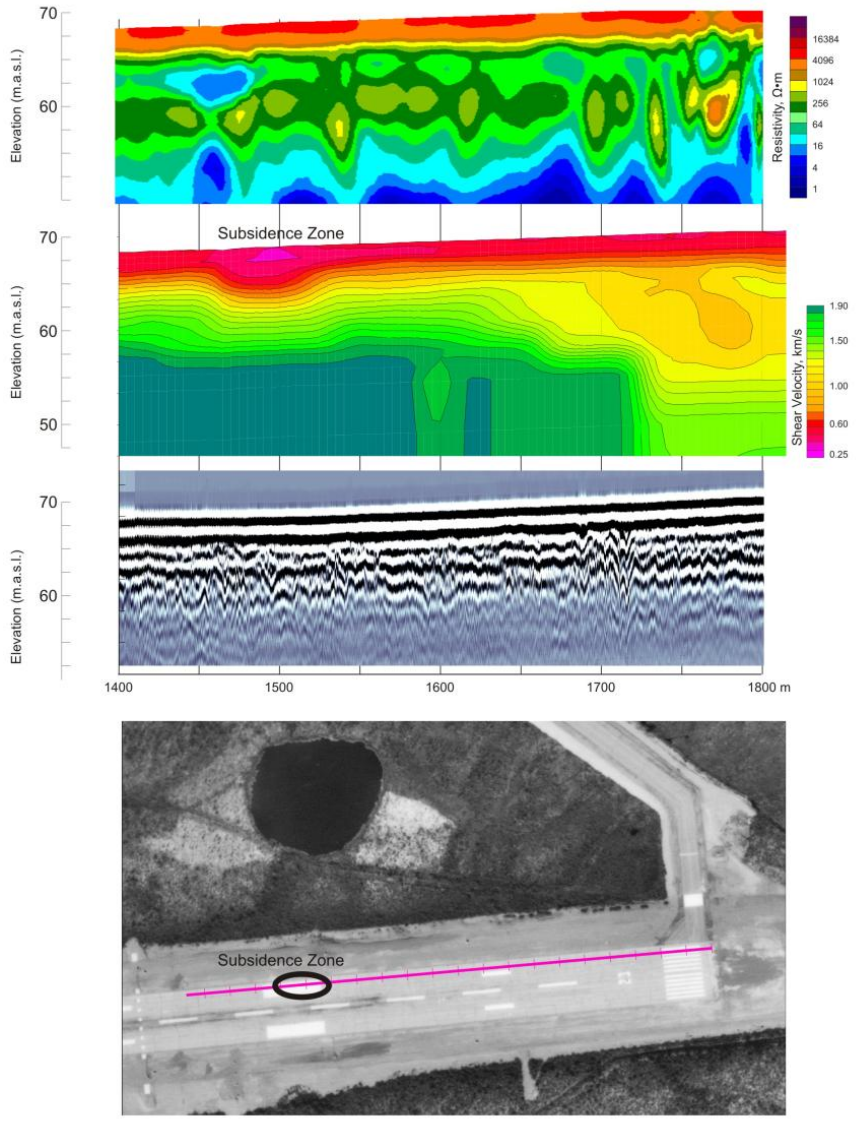

Figure 12- Three north-edge transects (resistivity, MASW, GPR) of the eastern 400 m of the runway (see also Figure 10). This area is of interest because of recent subsidence that has occurred near the northern edge of the runway, both at the 1000' marker (measured from E to W) and at the junction with the FOL taxiway.

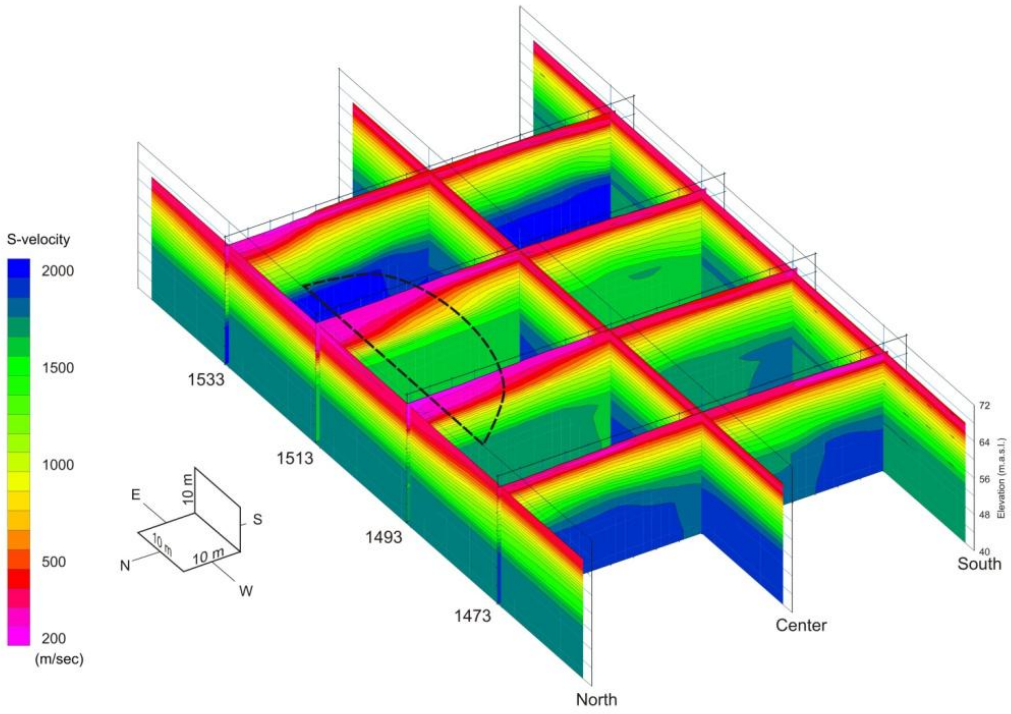

Figure 13 – (top) "2.5 D" fence diagram of the subsidence zone at the 1000' mark on the north edge of the Inuvik runway. The approximate surface 'footprint' of the disturbance is indicated by dashed line. (bottom) Surveying the subsidence zone, 300 m from the runway's eastern end.

Alpha and FOL Taxiways

Alpha taxiway is located within the same relict alluvial channel material as the eastern portion of the main runway (Figure 2). The taxiway and the western half of the apron have been subject to subsidence in the period following construction, but have been mostly stable for the last few decades. The pattern in the resistivity model (Figure 14) is similar to the eastern runway. There are a number of cables running under the taxiway and apron, but these are within the embankment layer. There is a deep resistive layer, probably continuous, that is likely ice-rich till. The GPR record shows collapse structures under the apron that are likely relicts from the earlier, post-construction period of subsidence. A similar structure can be observed in the historic GPR record of Judge *et al*. (1991). A portion of their record was obscured by noise from airport radio transmissions.

The MASW record shows relatively uniform, competent ground under the main runway, grading to a zone of slower seismic velocities along the taxiway toward the apron. This zone coincides with the anomalies in the resistivity record, suggesting potentially sensitive ground if the subsurface thermal regime were to change.

The record from the FOL taxiway (Figure 16) has a similar resistivity pattern, with deep anomalies again suggesting the presence of ice at depth. The GPR record highlights at least two disrupted sites within the subsurface – one beneath the concrete pad at the taxiway-runway junction (Figure 15) and the other situated halfway between the taxiway 'elbow' and the main runway.

The subsidence at the concrete pad is well known, and has been an on-going maintenance issue for the Forward Operating Location. Remedial steps were taken this summer (2011) to add fill and restore the concrete pad. The second site, roughly 100 m north of the main runway centerline, shows no surface expression, although there were cracks running the length of the taxiway which have been flagged as a concern. The historic GPR section of Judge et al. (1991) emphasizes the presence of ice wedges and icy sediments at this site, although it is not clear how the GPR record was interpreted here. The MASW data indicate slower S-wave velocities than the main runway, but not as slow as those under taxiway Alpha.

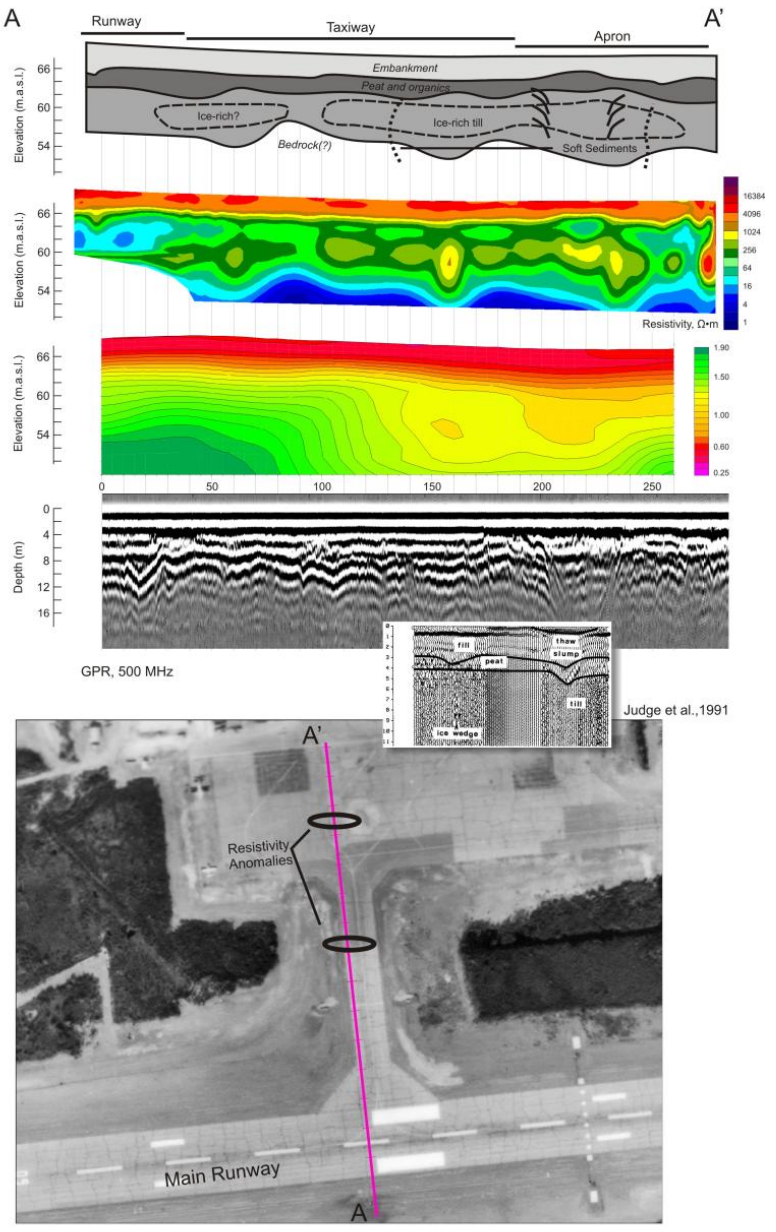

Figure 14- Alpha taxiway geophysical surveys: interpretation (top), OhmMapper resistivity profile, MASW shear velocity profile, GPR radargram, and aerial photo (bottom). Note comparison with Judge et al's 1991 GPR profiling (approximate match of scale and extent).

Figure 15- Looking northward from the main runway threshold to the FOL taxiway. The concrete pad in the foreground has subsided, but has recently been repaired (Summer, 2011).

Risk Assessment: Discussion

The use of two or more complimentary survey methods significantly improves our diagnostic capabilities on runways. An improved classification of terrain types, and potentially vulnerability, can be developed using a combination of resistivity (Ohm-Mapper), GPR and shear wave velocity (MASW) data. The combined set of tools provides an integrated picture of multiple properties of the subsurface materials. Low contrast amongst substrate-types may hinder diagnosis using one technique, but having the second technique will often improve the type discrimination.

In the context of permafrost studies, it should also be noted that resistivities and seismic velocities of ground materials change with temperature. There is likely to be improvement in the interpretation of survey data if there have been at least two surveys from different seasons (e.g. early spring and late summer/fall) when water phase changes may result in changes to the characteristic geophysical response of the substrate.

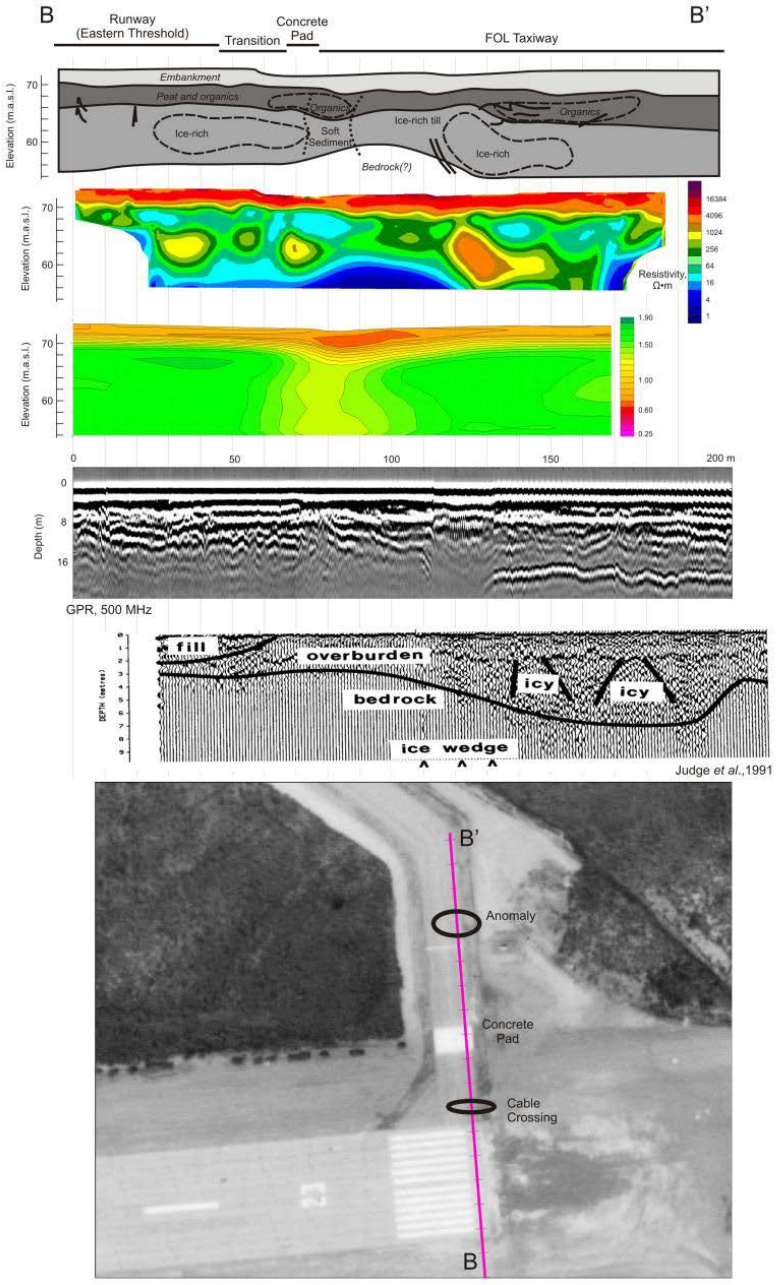

Figure 16- FOL Taxiway geophysical surveys: interpretation (top), OhmMapper resistivity profile, MASW shear velocity profile, GPR radargram, and aerial photo (bottom). Again, note comparison with Judge et al's 1991 GPR profiling (approximate match of scale and extent).

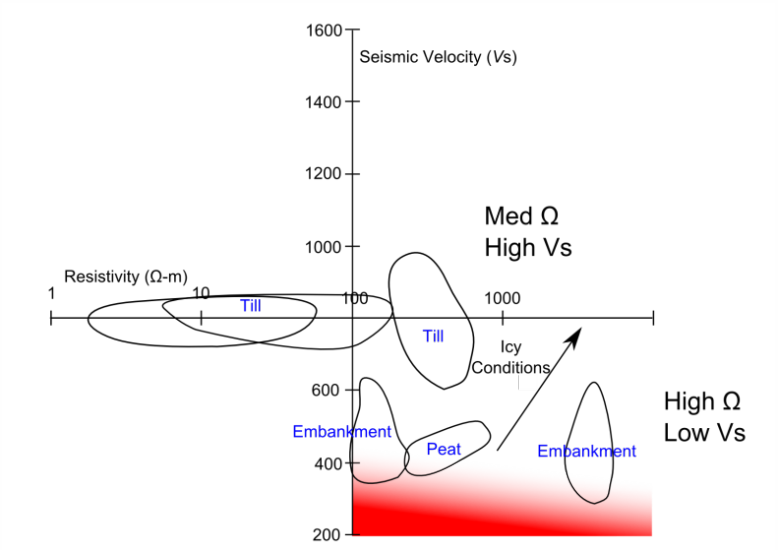

Figure 17- Geophysical 'domains', based on a biplot of resistivity and seismic velocity. Ellipses show the general location of clusters of values from multiple survey profiles. The red gradient indicates the general zone where surface subsidence was observed in the course of the survey work.

Figure 17 shows some representative resistivity and shear-velocity values of various substrate types, based on overlapping the model results from the OhmMapper and MASW surveys. Characteristic 'clusters' of points indicate the major seismic facies: embankment, till, and peat. These classifications depend, of course, upon the stratigraphic order (thus the relative density) of these units, which is invariant throughout the study area. Based on our observations of notable subsidence zones, as well as historic reports of subsidence, it is possible to assign some zones of probable risk within the biplot. These risk zones generally correspond to slower shear velocities and, to a lesser extent, lower resistivity values within each ellipse. Points within the risk zones should be highlighted for closer examination, including review of GPR records and field study. These sites may be associated with lower ice content, less competent substrate and – potentially - wetter conditions.

MASW results indicated that sites of notable subsidence were associated with shear wave velocities of 200-325 m/s within the embankment layer. This risk zone range may be higher within the deeper peat zone (300-400 m/s). Seismically 'slow' zones within the deeper strata may not require immediate attention if the embankment above appears competent and undistorted. They should be flagged as part of the assessment.

The estimated proportion of the runway sitting on ground ice can be calculated using the resistivity and GPR data in combination. In the course of data review, the presence of zones of high resistivity, inferred to be associated with ground ice, should be noted.

It will take more work to better calibrate the signatures of frozen versus unfrozen ground in the study area, but in general terms these methods hold promise for mapping vulnerable zones on runways. GPR provides additional confirmation by highlighting the geometry of underlying structures, and the galvanic resistivity provides a more robust verification of the range of site-specific resistivity values.

Conclusions and Recommendations

The Inuvik airport has proven to be a 'best-case scenario': the problem spots are clear, and the abundance of historic information and borehole records provides good verification of conclusions from the geophysical surveys. In order to further calibrate the interpretations made in this study, it would be highly desirable to carry out some further drilling work to confirm the observed stratigraphy and establish the ice content, particularly at the eastern end of the runway.

At Inuvik airport, resistivity surveys provide a basic distinction amongst the major stratigraphic units, and multi-channel analysis of surface waves (MASW) in combination with GPR provide several enhancements to these distinctions, as well as providing information on the competence and structure of the subsurface materials. There are good correlations with basic borehole data from the runway site. The geophysics imagery shows a relatively uniform subsurface along the principal runway, with some variation in peat thickness and depth to bedrock. The taxiways highlight problems associated with former drainage channels and lakes that were filled in during the course of construction. Three sites (Taxiway Alpha, FOL taxiway and a site at the east end of the main runway) showed evidence of historic disruption of the subsurface related to ground ice degradation. Ice rich zones could be identified with reasonable confidence based on resistivity and GPR profiles.

The combined datasets provide a means of identifying sites at risk, both in the immediate term and in the context of vulnerability to long-term trends in warming. A simple classification chart is proposed, in combination with other geophysical diagnostics, for assessing the overall risks presented by ground ice.

Inuvik runway has an intermediate to low risk rating. There has been substantial settling in the east, but things have stabilized. The recently patched subsidence zone at the 1000 ft marker will likely continue to be a problem since the imaged soft zone is significantly larger than the present surface expression. There is ongoing settlement in the west end, but this too will likely stabilize over time.

The remote sensing observations appear to fit well with the initial findings from the geophysics surveys. Relict drainage channels, identified by aerial photography, where peat and organics have accumulated over time, appear to be problem spots for ground subsidence. This linkage provides a promising indication that desktop assessment of aerial photographs and satellite images will help to target geophysics survey work, and minimize the time spent examining terrain that shows no indications of stability problems.

If the methods used here are to be applied at a broader scale (multiple runways), a targeted approach would help to minimize the person-hours of each survey. At this stage, we would recommend the use of at least the resistivity and surface wave analysis techniques. If terrain mapping of the site is completed before the geophysical survey, then the terrain suspected to be more susceptible could be prioritized in order to reduce survey hours.

The MASW technique is still evolving as a tool in engineering studies. It is anticipated that as the popularity of this technique grows, more sophisticated processing and interpretation techniques will become available. It could be coupled with reflection or refraction techniques to maximize the datasets available to assess the ground conditions. MASW works better on the paved runway surface than off runway, mostly likely due to poor coupling of the sledge hammer plate with the ground. Some further work on gravel runways will be needed to find the optimum result. Otherwise, the method holds great promise for work in permafrost areas. The OhmMapper and GPR should work well in either setting.

Some refinement of the data processing and interpretation technique is desirable. More experience on runways and on permafrost ground will help to address some of the uncertainties encountered in estimating subsurface conditions using the capacitavely-coupled resistivity and MASW data. Systematic evaluation of the many possible inversion model results will help to better constrain some of the uncertainty and guide interpretation.

Overall, the geophysics surveys provided a good integrated view of subsurface conditions, and offered an excellent opportunity to assess possible hazards related to infrastructure and warming ground conditions in the North. The data provide an important baseline that can be referred to in future investigations.

References

Calvert HT, Dallimore SR, Hunter JA. 2001. Application of geophysical techniques for mapping ice-bearing sediments, Mackenzie Delta, Western Arctic, Canada. In Proceedings of Conference on the Geophysical Detection of Subsurface Water on Mars, 6–10 August 2001. LPI Publication 1095: Houston, Texas; 7041.

dePascale GP, Williams KK, Pollard WH. 2008. Geophysical mapping of ground ice using a combination of capacitive coupled resistivity and ground penetrating radar, NWT, Canada. Journal of Geophysical Research – Earth Surface In press. DOI: 1029/2007JF000585

Geometrics. 2001. OhmMapper TR-1 Operations Manual. 29005-01 REV. F. 147 pp.

Geometrics. 2009. SeisImager Manual. Available from ftp.geometrics.com.

Hayashi, K. and Suzuki, H. 2004. CMP cross-correlation analysis of multi-channel surface-wave data. Exploration Geophysics. **35**: 7-13.

Hauck C, Kneisel C. 2008. Application of Capacitively-coupled and DC Electrical Resistivity Imaging for Mountain Permafrost Studies. *Permafrost and Periglacial Processes* 17: 169-177.DOI: 10.1002/ppp.555

Hauck C, Kneisel C. 2008. Applied Geophysics in Periglacial Environments. Cambridge University Press: Cambridge.

Henderson, J., n.d. report on the application of electrical and eletromagnetic techniques for use in the design and construction of northern pipelines. Associated Mining Consultants Ltd.

Hillbich C, Marescot L, Hauck C, Loke MH, and Mausbacker R. 2009. Applicability of electrical resistivity tomography monitoring to coarse blocky and ice-rich permafrost landforms. *Permafrost and Periglacial Processes*. 20(3): 269-284.

Hordt A, Hauck C. 2008. Electromagnetic methods. In Applied Geophysics in Periglacial Environments, Hauck C, Kneisel C (eds). Cambridge University Press: Cambridge.

Hunter, JA. 2007. Measurements of compressional and shear wave velocities and formation porosities in Quaternary sediments. Presented at OttawaGeo2007, Ottawa, Ontario 2007.

Judge AS, Tucker CM, Pilon JA and Moorman BJ. 1991. Remote sensing of permafrost by ground-penetrating radar at two airports in arctic Canada. *Arctic*. Vol. 4 Supp. 1. 40-48.

Knight R. 2001. Ground Penetrating Radar for environmental applications. *Annual Review of Earth and Planetary Science* **29**:229-55.

Loke MH. 1996. Tutorial: 2D and 3D electrical resistivity surveys. Lecture notes, Geotomo Software,

136 p.

Loke MH, Acworth I, Dahlin T. 2003. A comparison of smooth and blocky inversion methods in 2D electrical imaging surveys. *Exploration Geophysics.* **34**(3): 182-187.

Moorman1, B.J., Robinson, S.D., and Burgess, M.M. 2003. Imaging periglacial conditions with ground-penetrating radar. Permafrost and Periglacial Processes 14: 319–329. DOI: 10.1002/ppp.463

Park, C.B., Miller, R.D. and Xia, J. 1999. Multichannel analysis of surface waves. *Proceedings, 66th Annual Meeting of the Society of Exploration Geophysicists*. Denver, CO.

Park CB, Miller, RD. 2004. Roadside passive multichannel analysis of survey waves (MASW). *Journal of Environmental and Engineering Geophysics*. **13**: 1-11.

Park, CB, Miller, RD, Ryden N, Xia J, Ivanov J. 2005. Combined use of active and passive surface waves. *Journal of Environmental & Engineering Geophysics*. **10**(3): 323-334.

Todd BJ, Dallimore SR. 1998. Electromagnetic and geological transect across permafrost terrain, Mackenzie River delta, Canada. *Geophysics* **63**(6): 1914–1924.

Tunnicliffe J and Burn C. 2011. Preliminary terrain analysis: Inuvik (Mike Zubko, CYEV) and Déline (CYWJ) Airports. Report submitted to the Department of Transportation, GNWT. Carleton University Department of Geography and Environmental Studies. 21 pp.

Yoshikawa K, Leuschen C, Ikeda A, Harada K, Gogineni P, Hoekstra P, Hinzman L, Sawada Y, Matsuoka N. 2006. Comparison of geophysical investigations for detection of massive ground ice (pingo ice). *Journal of Geophysical Research* 111(E6): DOI:10.1029/2005JE002573.

Xia J, Miller RD, Park CB. 1999. Estimation of near-surface shear-wave velocity by inversion of Rayleigh waves. *Geophysics*. **64**(3): 691-700.

Xia J, Miller RD, Park CB, Ivanov J, Tian G, Chen C. 2004. Utilization of high-frequency Rayleigh waves in near-surface geophysics. The Leading Edge. August, 2004: 753-759.

Zimmerman RW, King MS. 1986. The effect of freezing on seismic velocities in unconsolidated permafrost. *Geophysics* **51**: 1285–1290.